JOURNAL OF MATERIALS SCIENCE 21 (1986) 1275–1279

A new metastable phase near 60 at % Zr from amorphous Ni–Zr

D. S. EASTON, C. G. McKAMEY, D. M. KROEGER, O. B. CAVIN
Metals and Ceramics Division, Oak Ridge National Laboratory, Oak Ridge, Tennessee 37831, USA

Metallic glass alloys of Ni–Zr were prepared by vapour and liquid quenching. For glass compositions at and near 60 at % Zr, crystallization proceeded by the sequence: amorphous → metastable crystalline phase → $NiZr_2$ + NiZr. The metastable $Ni_{40}Zr_{60}$ phase exhibited a very distinctive X-ray diffraction pattern and was present in both liquid- and vapour-quenched samples. Long-term anneals of samples with the metastable structure produced the equilibrium phases $NiZr_2$ and NiZr. The crystallization of the amorphous structure directly to a single metastable phase shows a correspondence between the compositions of the amorphous and crystalline phases. These results thus suggest a connection between the short-range structure of the glassy phase and the crystalline phases to which they transform. An observation of peaks and valleys in a plot of the X-ray scattering vector, Q_p, against glass composition is noted.

1. Introduction

A number of studies have been undertaken on the crystallization behaviour and kinetics of Ni–Zr metallic glasses [1–14]. Interest in the system is due to the fact that glasses may be found over a wide composition range and that small variations in composition produce large differences in the crystallization process.

Buschow *et al.* [11] found a large exothermic transition by differential scanning calorimetry (DSC) in $Zr_{1-x}Ni_x$ and $Hf_{1-x}Ni_x$ alloys in compositions slightly below $x = 0.4$ but did not find corresponding X-ray diffraction (XRD) lines that matched the transition. They suggested either the occurrence of an atomic rearrangement within the amorphous state or a partial conversion into a crystalline precipitate. It has since been proposed [3, 9] that this first DSC peak is due to precipitation of crystallites or clusters too small to be detected by diffraction techniques. McKamey *et al.* [1] found that DSC scans of a $Ni_{41}Zr_{59}$ glass showed a single peak corresponding to formation of the new phase described in this work followed by a high-temperature peak for the transformation of the metastable phase to the equilibrium phases of NiZr and $NiZr_2$. Metastable phases were found in nickel-rich alloys by Dong *et al.* [10], in $Ni_{64}Zr_{36}$ by Polesya and Slipchenko [14], and in $Ni_{22}Zr_{78}$ by Buschow and Beekmans [13].

Altounian *et al.* [8] found complex intermediate exotherms by DSC for a $Ni_{40}Zr_{60}$ alloy. However, XRD studies showed only a glassy phase plus $NiZr_2$ in the intermediate stages and the equilibrium phases NiZr and $NiZr_2$ after heating to 900 K. In the same study, a new Ni_2Zr peritectoid phase was reported.

In the present work a new low-temperature crystalline phase has been found at $Ni_{40}Zr_{60}$ that transforms into $NiZr_2$ and NiZr when heated to higher temperatures or held for rather long times at low temperatures. The presence of this phase has not been reported in any previous studies that the authors are aware of.

Buschow [4] and Dong *et al.* [10] found that, for as-quenched samples, values of the X-ray scattering vector Q_p (where $Q_p = 4\pi \sin\theta/\lambda$) of the principal peak show two near-linear regions intersecting roughly at 45 at % Zr. We propose that a plot of Q_p against composition shows a series of short cycles that are related to both the equilibrium and metastable crystalline states.

2. Experimental details

Metallic glass alloys of Ni–Zr were prepared by electron-beam evaporation, splat quenching, and melt spinning. The amorphous structure was found in thin film (0.1 to 1.0 μm) vapour quenched alloys between 18 and 77 at % Zr. Alloys at 5 and 93 at % Zr were crystalline in the as-deposited state. Liquid-quenched samples (20 to 30 μm thick) were made from arc-melted buttons by an arc-hammer apparatus and by melt spinning on a 0.051 m thick, 0.305 m diameter copper wheel at a surface speed of 25 m sec^{-1} in a helium atmosphere. Compositions were monitored by careful weight measurements of the alloy buttons and by energy dispersive X-ray fluorescence (EDXF). Accuracy is estimated to be within 0.2 at %.

Preliminary XRD scans were made on a Philips spectrometer and later detailed analysis was conducted on a fully automated Philips powder diffractometer (APD 3600) utilizing Cu$K\alpha$ radiation ($\lambda = 0.154\,051$ nm).

DSC measurements were used to study the crystallization kinetics and will be reported elsewhere [1]. Samples were heat treated either in the DSC under flowing argon, in a dynamic vacuum system, or in sealed evacuated quartz capsules after wrapping in zirconium and tantalum foil envelopes. Yttrium

0022–2461/86 $03.00 + .12

powder was placed in the capsules for gettering. The capsules were placed in a standard tube furnace for the static anneals.

3. Results and discussion

Unless noted otherwise, the composition of samples discussed in this work is $Ni_{40}Zr_{60}$. Evaporated films taken to 1000 K in the DSC showed no crystallization peaks and XRD indicated an amorphous structure still existed. We believe that the argon environment in the DSC is not of sufficient quality to prevent some oxidation of the $\sim 0.2\,\mu m$ thick films. Anneals of the films in capsules were more successful although crystallization still occurred more than 100 K higher than in the liquid-quenched samples. We did not determine whether this was due to oxidation, to some unique property of the vapour-quenched samples, or to an effect of sample thickness on nucleation and growth of crystallites.

Examination of a large number of XRD traces of splats, ribbons, and films showed a characteristic pattern of four major peaks for samples annealed around 700 K. Fig. 1 shows a series of XRD traces after annealing a series of liquid-quenched ribbon samples for 20 min at various temperatures. The major peak of the new phase is seen at $2\theta = 38.6°$. The crystallization proceeds from the amorphous state at 683 K to amorphous plus metastable states at 693 K. The new phase is well defined at 703 K. Samples with the metastable structure were examined extensively by transmission electron microscopy (TEM) to establish that they consisted of single-phase material only. No other phases were found in any of the samples annealed to produce the metastable phase. At progressively higher temperatures the peaks associated with the new phase slowly disappear and are replaced by the equilibrium phases, $NiZr_2$ and NiZr. The major peak of the new phase is completely gone by 773 K. Between 873 and 973 K there is a strong increase in the intensity of the major peaks of $NiZr_2$ and NiZr. The pattern as shown at 703 K was seen in all samples heated to above the first DSC exotherm or furnace annealed at temperatures of ~ 700 K. The development of the equilibrium phases at intermediate temperatures is rather unusual in that the major intensity lines do not appear initially and the relative intensities are not what would be expected for the two phases. Table I lists the d spacings and relative intensity values (observed and literature values for $NiZr_2$, tetragonal Al_2Cu type, and NiZr, orthorhombic CrB type [15, 16]) of samples annealed at 973 K (equilibrium) and 703 K (metastable). Although there is overlap in some instances, as might be expected, the d spacings clearly indicate the differences in the new phase and the equilibrium phases. Peaks at $d = 0.259$ and 0.236 nm were not identified but are assumed to be related to Ni–Zr since no significant impurities were found in any of the samples. The new phase was the

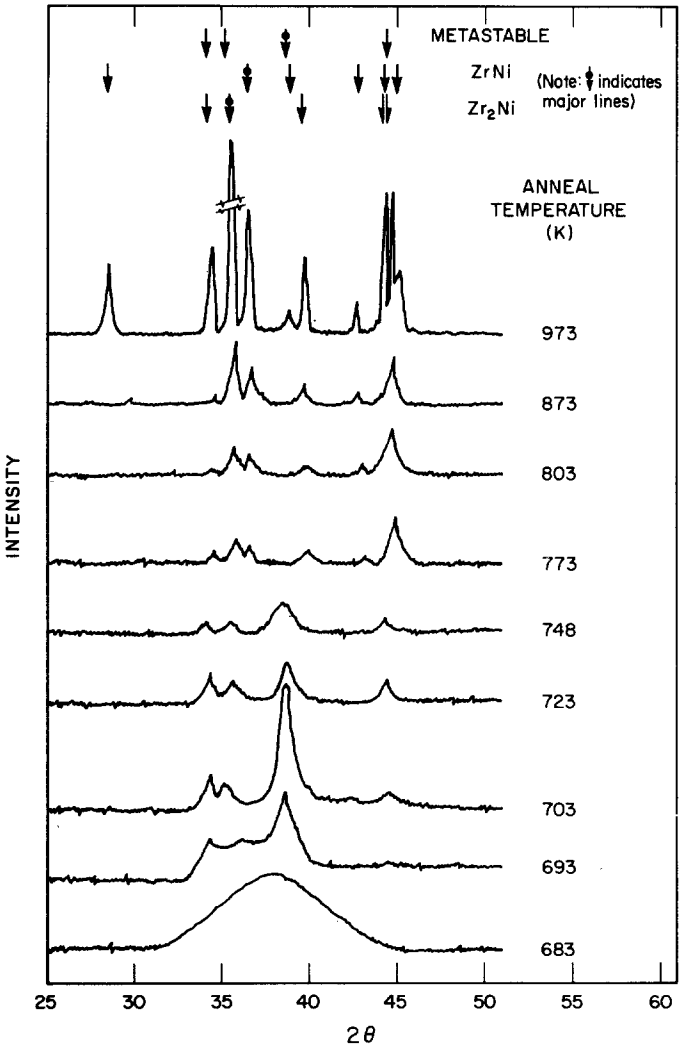

Figure 1 X-ray diffraction spectra of $Ni_{40}Zr_{60}$ samples annealed at varying temperatures showing the progression: amorphous → metastable → $NiZr_2$ + NiZr.

TABLE I X-ray diffraction results

Literature values [15, 16]				Annealed 973 K (equilibrium) observed		Annealed 703 K (metastable) observed	
NiZr		$NiZr_2$					
d (nm)	I	d (nm)	I	d (nm)	I	d (nm)	I
0.313	10	–	–	0.315	13	–	–
		0.262	10	0.262	27	0.262	31
–	–	–	–	0.259	35	–	–
–	–	0.253	100	0.253	100	0.253	38
0.246	100	–	–	0.247	53	–	–
–	–	–	–	0.236	3	–	–
–	–	–	–	–	–	0.234	100
0.231	20	–	–	0.232	8	–	–
–	–	0.228	10	0.228	29	–	–
0.211	18			0.212	12	–	–
0.204	25	0.205	60	0.205	68	–	–
–	–	–	–			0.203	37
0.202	44	–	–	0.202	19	–	–
–	–	–	–	–	–	0.186	3
–	–	–	–	–	–	0.175	6
0.162	14	–	–	0.163	7	–	–
0.158	16	–	–	0.158	12	–	–
0.153	16	0.153	10	0.153	16	0.153	15
–	–	0.150	60	0.150	35	0.150	18
0.144	2	0.1449	20	0.1449	6	–	–
		0.138	40	0.138	10	–	–
0.136	8	–	–	–	–	0.135	7
–	–	0.132	50	0.132	24	–	–
–	–	–	–	–	–	0.131	14
0.128	20	–	–	0.128	8	–	–
0.125	8	–	–	0.125	7	–	–
–	–	0.117	70	0.117	16	0.117	8
–	–	–	–	–	–	0.099	26

TABLE II Heat-treatment results

$Ni_{1-x}Zr_x$	Sample type	Anneal			Structure
		Type	Time (min)	Temperature (K)	
60	Ribbon	Salt bath	10	645	Amorphous
60	Ribbon	Salt bath	18	690	Metastable
60	Ribbon	Salt bath	15	693	Metastable
60	Ribbon	Salt bath	20	695	Metastable
60	Ribbon	Salt bath	10	699	Metastable
60	Ribbon	Quartz capsule in salt bath	10	645	Amorphous
60	Ribbon	Quartz capsule in salt bath	15	693	Metastable
60.1	Splat	Quartz capsule	45	733	$NiZr_2$ + metastable
60.1	Splat	Quartz capsule	45	783	$NiZr_2$ + NiZr
~65	Thin film	Quartz capsule	45	683	Amorphous
~65	Thin film	Quartz capsule	45	733	Amorphous
~65	Thin film	Quartz capsule	45	783	Amorphous + metastable
~65	Thin film	Quartz capsule	45	833	Metastable
60	Ribbon	Dynamic	30	678	Amorphous
60	Ribbon	Dynamic	60	678	Amorphous
60	Ribbon	Dynamic	5	683	Amorphous
60	Ribbon	Dynamic	15	683	Amorphous
60	Ribbon	Dynamic	110	683	Amorphous + metastable
60	Ribbon	Dynamic	20	693	Amorphous + metastable
60	Ribbon	Dynamic	20	703	Metastable
60	Ribbon	Dynamic	20	723	Weak metastable
60	Ribbon	Dynamic	20	748	Weak metastable
60	Ribbon	Dynamic	20	773	$NiZr_2$ + NiZr*
60	Ribbon	Dynamic	20	803	$NiZr_2$ + NiZr
60	Ribbon	Dynamic	20	873	$NiZr_2$ + NiZr
60	Ribbon	Dynamic	50	873	$NiZr_2$ + NiZr
60	Ribbon	Dynamic	20	973	$NiZr_2$ + NiZr
60	Ribbon	Dynamic	120	973	$NiZr_2$ + NiZr
60	Ribbon	Dynamic	30 h	673	Metastable
60	Ribbon	Quartz capsule	285 h	703	$NiZr_2$ + NiZr
60	Ribbon	Quartz capsule	285 h	673	Metastable + $NiZr_2$ + NiZr

*Diffraction line intensities not consistent with equilibrium spectra.

only one found in samples heated to 700 K for 30 h. There were still some remnants of the phase present, together with $NiZr_2$ and NiZr, after heating to 680 K for 285 h; however, the phase had disappeared after heating at 700 K for 285 h.

Table II summarizes the results of anneals of various types of samples. Samples immersed directly into a salt bath and then quenched had a glossy black coating. When the coating was removed, XRD showed the metastable phase present in samples heated at 700 K.

The peaks in XRD patterns of the metastable crystalline phase were much sharper after 90 min and 30 h anneals at 703 K. The sharpening apparently is due to grain growth and led to an initial conclusion that the new phase was probably a low-temperature equilibrium phase. However, the fact that the phase is replaced by the equilibrium phase after long time anneals indicates that it is indeed metastable in nature. Since the samples prepared and annealed in various ways all showed the characteristic four-peak diffraction pattern, the new phase appears to be a result of nickel–zirconium interaction and not due to preparation and heat-treatment methods.

Long-term X-ray exposures using the Debye–Scherrer powder technique have produced a large number of diffraction peaks associated with the new phase. Work is underway using this method along with electron beam diffraction, to identify the structure.

Kroeger *et al.* [5, 6] noted a minimum in the enthalpy change upon crystallization at ~58 to 59 at % Zr, and a maximum at ~60 at % Zr in the density of electronic states at the Fermi level, $N(E_f)$, as determined from low-temperature specific heat measurements. Two superconducting transitions were found for some compositions indicating the coexistance of two amorphous phases. Estimates of the compositions of the two phases, based on previous superconducting transition temperatures against composition data, were 60 and 67 at % Zr. Compositions near 66.7 at % Zr crystallize polymorphically to the equilibrium compound $NiZr_2$. With the discovery that samples with compositions near 59 to 60 at % Zr crystallize directly to a single metastable phase, correspondence has been demonstrated between the composition of amorphous and crystalline phases in this composition range. These results suggest a connection between the short-range structures of these amorphous phases and the crystalline phases to which they transform.

Frahm *et al.* [2], using extended X-ray absorption fine structure (EXAFS) measurements, found that a Ni–Zr bond length of 0.275 nm for crystalline $Ni_{33}Zr_{67}$ was shortened to 0.262 nm in the amorphous state. The work indicated a chemical bonding between unlike atoms resulting from a charge transfer from zirconium to nickel. This bonding between zirconium and nickel atoms pointed to the probability that some kind of molecular unit is present in the glass. It was concluded by comparing coordination numbers that although the units were consistent with $NiZr_2$ molecules (with some larger units also), the measured distances indicated that they were not exactly the square antiprism found in the $NiZr_2$ crystal. Phase separation has also been shown by Schulz *et al.* [3] and van Swijgenhoven *et al.* [9].

In related work on this system an observation is noted concerning the X-ray scattering vector, Q_p. This value is obtained from the position of the principal diffuse diffraction peak in the amorphous samples by the term $4\pi \sin\theta/\lambda$ (λ is wavelength of the radiation used) and is related to the distance between the nearest-neighbour atoms at least to a first approximation. Buschow [4] and Dong *et al.* [10] found that a plot of Q_p against composition resulted in two near-linear curves intersecting between 40 and 50 at % Zr. The values of Q_p obtained in the present work are shown plotted against zirconium composition in Fig. 2. A series of peaks and valleys occur which seem to be too regular to be attributed to scatter. The peaks coincide with zirconium compositions near the metastable phase, the eutectic, and $NiZr_2$. It must be emphasized, however, that these data are preliminary

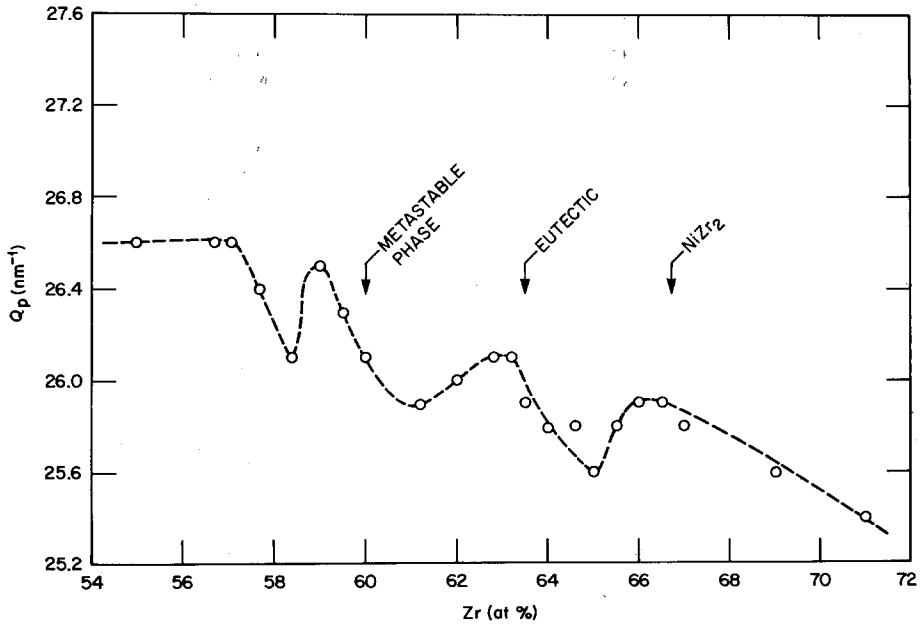

Figure 2 The X-ray scattering vector, Q_p, plotted against zirconium composition for a range of amorphous Ni–Zr alloys. $Q_p = 4\pi \sin\theta/\lambda$.

and must be investigated further before a more definitive analysis is made. More precise Q_p values obtained from radial distribution functions using very long X-ray exposures will be made in the future. It is probable that the deviations in Q_p values may reflect abrupt changes in the chemical short-range order (CSRO) for compositions within this range. Composition-dependent CSRO has been seen in many studies [1–9, 11]. Other investigators have found unexplained occurrences in DSC curves [7, 8] and in the enthalpy, ΔH, and $N(E_f)$ [5, 6] at compositions close to 60 at % Zr. The formation of the new phase found in this work at such a low temperature suggests that clusters of atoms with the composition $Ni_{40}Zr_{60}$ probably existed in the amorphous glass and possibly acted as nucleation sites for the initial crystallization.

Acknowledgements

The authors wish to thank J. O. Scarbrough for preparation of the alloys, J. A. Horton for TEM examination and Gwendolyn Sims for typing the manuscripts. This research was sponsored by the Division of Materials Science, US Department of Energy under contract DE–AC05–840R21400 with the Martin Marietta Energy Systems Inc.

References

1. C. G. McKAMEY, D. M. KROEGER, D. S. EASTON and J. O. SCARBROUGH, to be published.
2. R. FRAHM, R. HAENSEL and P. RABE, *J. Phys. F Met. Phys.* **14** (1984) 1333.
3. R. SCHULTZ, V. MATIJASEVIC and W. L. JOHNSON, *Phys. Rev. B* **30** (1984) 6856.
4. K. H. J. BUSCHOW, *J. Phys. F Met. Phys.* **14** (1984) 593.
5. D. M. KROEGER, C. G. McKAMEY and J. O. SCARBROUGH, *J. Non-Cryst. Solids* **61/62** (1984) 937.
6. D. M. KROEGER, C. C. KOCH, J. O. SCARBROUGH and C. G. McKAMEY, *Phys. Rev. B* **29** (1984) 1199.
7. K. H. J. BUSCHOW, I. VINCZE and F. VAN DER WOUDE, *J. Non-Cryst. Solids* **54** (1983) 101.
8. Z. ALTOUNIAN, TU GUO-HUA and J. O. STROMOLSEN, *J. Appl. Phys.* **54** (1983) 3111.
9. H. VAN SWIJGENHOVEN, L. M. STALS and K. H. J. BUSCHOW, *Phys. Status Solidi* **72** (1982) 153.
10. Y. D. DONG, G. GREGAN and M. G. SCOTT, *J. Non-Cryst. Solids* **43** (1981) 403.
11. K. H. J. BUSCHOW, B. H. VERBEEK and A. G. DIRKS, *J. Phys. D Appl. Phys.* **14** (1981) 1087.
12. M. G. SCOTT, G. GREGAN and Y. D. DONG, Proceedings of the 4th International Conference on Rapidly Quenched Metals, edited by T. Masamoto and K. Suzuki, (The Japan Institute of Metals, Sendai, 1981) pp. 671–4.
13. K. H. J. BUSCHOW and N. M. BEEKMANS, *Phys. Rev. B* **19** (1979) 3843.
14. A. F. POLESYA and L. S. SLIPCHENKO, *Russ. Met.* **6** (1973) 103.
15. Powder Diffraction File, Sets 19–20, Card No. 19-857, (JCPDS, Swarthmore, Pennsylvania, 1979).
16. *Idem*, Sets 11–15, Card No. 12–478, (JCPDS, Swarthmore, Pennsylvania, 1972).

Received 16 April
and accepted 7 June 1985